Corrigendum to Atmos. Meas. Tech., 14, 5415–5428, 2021
https://doi.org/10.5194/amt-14-5415-2021-corrigendum

Atmospheric Measurement Techniques
Open Access
EGU

Corrigendum to "Validation of Aeolus winds using ground-based radars in Antarctica and in northern Sweden" published in Atmos. Meas. Tech., 14, 5415–5428, 2021

Evgenia Belova[1], Sheila Kirkwood[1], Peter Voelger[1], Sourav Chatterjee[2], Karathazhiyath Satheesan[3], Susanna Hagelin[4], Magnus Lindskog[4], and Heiner Körnich[4]

[1]Swedish Institute of Space Physics, Kiruna, 98128, Sweden
[2]National Centre for Polar and Ocean Research, Ministry of Earth Sciences, Vasco da Gama, Goa, 403804, India
[3]Department of Atmospheric Sciences, School of Marine Sciences, Cochin University of Science and Technology, Cochin, Kerala, 682 016, India
[4]Swedish Meteorological and Hydrological Institute, Norrköping, 60176, Sweden

Correspondence: Evgenia Belova (evgenia.belova@irf.se)

Published: 11 May 2022

In the data analysis presented in Belova et al. (2021), due to a software error that was found after publishing the paper, the heights of radar (and ERA5 model) winds were on some occasions not correctly matched with the heights of the Mie cloudy winds measured by the lidar on Aeolus.

In the case of the winds from the ESRAD radar 21 % of the heights were mismatched for the descending orbits and 18 % for the ascending passes, but the average height differences were small (mean mismatch – 440 m for descending passes, – 385 m for ascending; i.e. the Mie winds were compared with ESRAD winds from, on average, slightly higher heights). The changes in correlation, slope and bias parameters (Table 5, new version provided here) for both descending and ascending passes are small and within the uncertainties of the original version. Standard deviations are now slightly smaller: 3.2–4.2 m s^{-1} (compared to 3.9–5.5 m s^{-1} originally). Changes in the related figures are very small and not statistically significant.

In the case of the winds from the MARA radar (Figs. 6–9 and Table 3, new versions provided here), 18 % of the heights were mismatched for the descending tracks (mean mismatch 250 m) and 100 % for the ascending tracks (mean mismatch 2200 m); i.e. the Mie winds were compared with MARA winds from lower heights. The changes in comparison parameters (Table 3) for the descending passes are small and within the uncertainties of the original version. For the ascending passes, where the height mismatch was large and systematic, there is a significant change in the bias, and this is apparent in the related updated Figs. 6, 7, 8 and 9b. The changes are largest for summer, ascending tracks (Figs. 6b, 8, 9b and 9d). The correction has removed the large bias which was previously reported for these tracks. The corrected bias is not significantly different from zero.

As a result of these corrections the sentence in the Abstract "A robust significant bias of 7 m s^{-1} is found for the Mie winds for the ascending tracks at MARA in summer" should be ignored, as should the discussion of this (incorrect) bias in the Sect. 4.1 and in the Summary and Conclusion.

The new updated versions for Figs. 6, 7, 8, 9b, d, f and Tables 3 and 5 are on the next pages.

Table 3. Aeolus Mie–MARA horizontally projected line-of-sight (HLOS) wind comparison.

Aeolus Mie vs. MARA	Summer 24 September–31 December 2019		Winter 1 July–23 September 2019	
	ascend	descend	ascend	descend
Altitudes, km	0.8–6.5		1.5–3.7	
N points	33	37	14	10
correlation	0.60	0.74	0.79	0.55
Slope, 95 % conf. interval	1.0 [0.7 1.4]	1.0 [0.7 1.3]	1.0 [0.5 1.4]	0.8 [−0.2 1.8]
Intercept, m s^{-1}	−0.9	0.6	−2.5	2.2
Bias, m s^{-1} 90 % conf. interval	−0.7 [−2.8 1.4]	1.3 [0.0 2.6]	−2.1 [−4.0 −0.2]	0.2 [−2.7 3.2]
SD, m s^{-1}	7.1	4.9	3.9	5.1

Table 5. Aeolus Mie–ESRAD HLOS wind comparison.

Aeolus Mie vs. ESRAD	Summer 1 July–23 September 2019		Winter 24 September–31 December 2019	
	ascend	descend	ascend	descend
Altitudes, km	2.5–10.9		2.4–10.9	
N points	33	79	36	57
Correlation	0.82	0.92	0.93	0.90
Slope, 95 % conf. interval	0.8 [0.6 0.9]	0.8 [0.8 0.9]	1.1 [1.0 1.2]	0.9 [0.8 1.0]
Intercept, m s^{-1}	0.8	0.3	2.4	0.3
Bias, m s^{-1} 90 % conf. interval	0.2 [−1.0 1.4]	1.2 [0.4 2.0]	2.5 [1.6 3.4]	0.9 [0.0 1.8]
SD, m s^{-1}	4.1	4.2	3.2	4.1

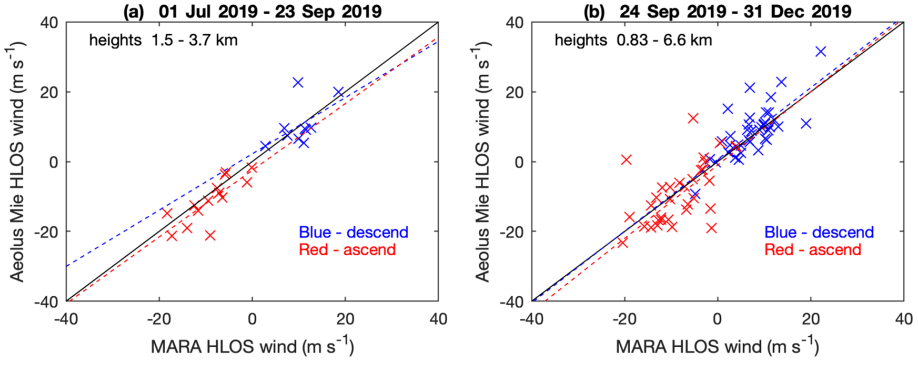

Figure 6. Scatter plots of Aeolus Mie HLOS winds against HLOS winds according to MARA radar data. Red crosses indicate measurements made on ascending tracks, blue crosses those on descending tracks. Dashed red and blue lines show fitted regression lines. Black dashed line indicates equality. Heights indicated are the lowest and highest where valid winds are available for comparison. Panel **(a)** is for the Antarctic winter period 1 July–23 September 2019, and **(b)** is for summer 24 September–31 December 2019.

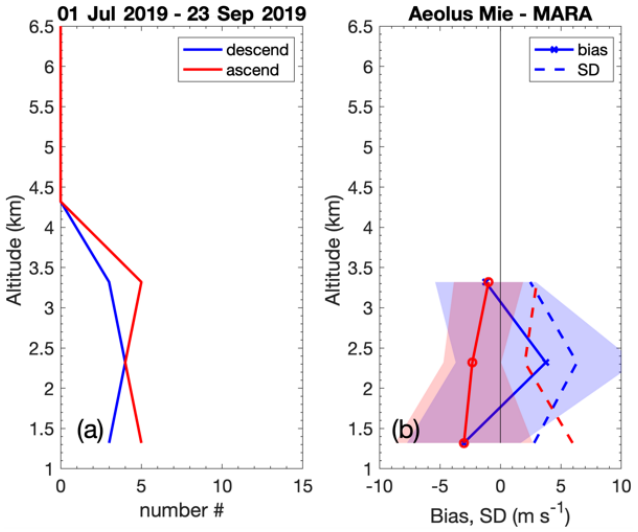

Figure 7. Height profiles in 1 km bins of **(a)** the number of comparison points available and **(b)** mean value (bias) and standard deviation of the differences between Aeolus Mie HLOS winds and MARA-derived HLOS winds for the Antarctic winter period 1 July–23 September 2019. Red lines and shading are for ascending tracks, and blue is for descending ones. Solid lines in **(b)** show the bias, with the shaded areas corresponding to the 90 % confidence interval. Dashed lines in **(b)** show the standard deviation.

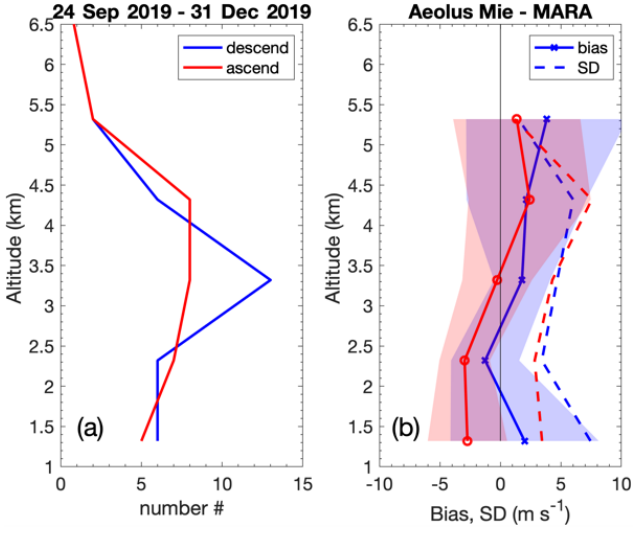

Figure 8. The same as Fig. 7 but for the Antarctic summer period 24 September–31 December 2019.

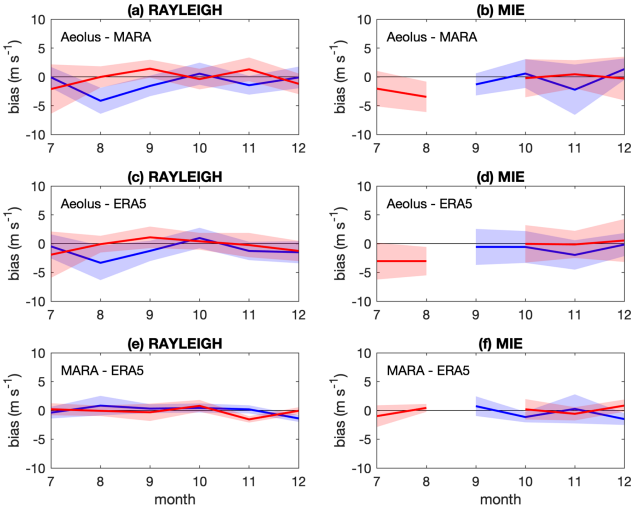

Figure 9. Month-by-month mean values of biases in HLOS winds (solid lines) and 90 % confidence limits (shaded areas) at MARA. Red is for ascending tracks, and blue is for descending ones. **(a)** Aeolus Rayleigh minus MARA; **(b)** Aeolus Mie minus MARA; **(c)** Aeolus Rayleigh minus ERA5; **(d)** Aeolus Mie minus ERA5; **(e)** MARA minus ERA5 at available Aeolus Rayleigh comparison times and heights; **(f)** MARA minus ERA5 at available Aeolus Mie comparison times and heights.